Chapter Five

Single Kink Dynamics in a Easy-Plane Antiferromagnet

5.1 Easy-Plane Antiferromagnets

Here the properties of nonlinear kink modes in a 1-D easy-plane classical antiferromagnet are studied (see also Wysin et al. 1985), especially to make a comparison to the kink modes in the ferromagnet. The same Hamiltonian is used, but the sign of the nearest neighbor exchange is reversed,

$$H = \sum_n \{J\vec{S}_n \cdot \vec{S}_{n+1} + A(S_n^z)^2 - g\mu_B \vec{B} \cdot \vec{S}_n\} \quad . \tag{5-1}$$

Here J and A are positive; again the xy plane is the easy plane. The applied field is taken to be in the x-direction; $\vec{B} = B\hat{x}$.

There are some real materials which are believed to be described by this Hamiltonian, most notably the spin S = 5/2 compound $(CH_3)_4)NMnCl_3$, tetramethyl ammonium manganese chloride, or TMMC for short. For this compound, JS^2 = 85 K and AS^2 = 2 K, and g = 2.0 (Boucher et al. 1981).

The crystal structures of TMMC has been determined by Morosin and Graeber (1967) using x-ray diffraction to be hexagonal with a = 9.151 Å, c = 6.494 Å. It is believed to be centrosymmetric $P6_3/m$ with the $(CH_3)_4N^+$ ions located at random positions between the $MnCl_3^-$ chains. There are two formula units per unit cell. The structure is reminiscent of the $CsNiF_3$ structure; both have the general form ABX_3, where $A = C_s^+$ or $(CH_3)_4N^+$, $B = Ni^{2+}$ or Mn^{2+}, and $X = F^-$ or Cl^-. The Cl^- ions form a cage for the magnetic Mn^{2+} ions and provide the superexchange paths between them. A given Mn^{2+} ion is surrounded by six Cl^- ions located at the vertices of a trigonally distorted octahedron. The Mn-Mn separation is a_0 = 3.25 Å along the chains and 9.15 Å between chains; the structure itself is

largely responsible for the 1-D nature of the material.

The exchange constant J was first estimated experimentally by fits to the high T susceptibility measurements of Dingle et al. (1969), and later by inelastic neutron scattering (Hutchings et al. 1972); the presently accepted value is $J = 6.6 \pm 0.15$ K. The exchange between chains is of the order of 10^{-3}K (Hutchings et al. 1972), and can be related to the transition to a 3-D ordered state at $T_N = 0.84$ K (Dingle et al. 1969). This phase transition is also seen in the specific heat measurements of Dietz et al. (1974).

Any anisotropy due to crystal fields in negligible; however, there is a small ($\sim$ 1.6%) easy-plane anisotropy of dipolar origin. Walker et al. (1972) suggested that the anisotropy constant A in Hamiltonian (5-1) can be written $A = 3g^2\mu_B^2/a_0^3$ with $g = 2.0$. Neutron inelastic scattering experiments by Heilmann et al. (1979) verified that this is correct by measuring the effect of the dipolar anisotropy on the gap in the zone boundary spin waves (an optical out-of-plane mode to be discussed below). These measurements also verified the existence of another mode (in-plane) whose gap energy is proportional to the field applied in the easy plane.

Further neutron scattering experiments (Boucher et al. 1979) where the correlation length was measured have shown that TMMC is essentially described by an XY model below 5 K, consistent with the earlier predictions of Walker et al. (1972) that the anisotropy becomes important starting below 20 K. Therefore, in the temperature range $5 < T < 20$ K we expect Hamiltonian (5-1) is necessary to describe TMMC. The model is intermediate between the isotropic Heisenberg model and the XY model, and the finite anisotropy is expected to have important effects on the dynamics.

5.2 In-Plane and Out-of-Plane Linear and Nonlinear Modes

Neutron scattering experiments (Heilmann et al. 1979) have measured the dispersion relations for small amplitude (linear) spin waves, as well as studying the properties of the nonlinear kink excitations (rotations through π of spin vectors) which are possible (Boucher et al. 1980, Reguault et al. 1982). A spin wave analysis shows that there are two branches, or modes, possible: oscillations predominantly in the easy plane (in-plane) and oscillations predominantly out of the easy plane (out-of-plane). Similarly it has been pointed out (Harada et al. 1981) that there are two nonlinear kink modes possible. The first is an in-plane, or xy kink, where the spins rotate through π in the easy plane, around the anisotropy axis, with only small z-components (Mikeska 1980, Maki 1980). Since the spins must point against the applied field, the energy depends on the field, and statically is equal to $g\mu_B BS$. The second is an out-of-plane, or yz kink, where the spins rotate through π out of the easy plane, around the field, with only small x-components. The spins point against the anisotropy field, and therefore the kink energy depends on A. Static yz kinks have energy $(8AJS^4)^{1/2}$. At a critical field $B_c \equiv (8AJS^2)^{1/2}/g\mu_B$, the two energies are equal; for TMMC this field is $B_c \simeq 100$ kG. At low fields $B < B_c$, the xy kink has the lower energy, while at high fields the yz kink has the lower energy. Thus one expects that thermal kink-antikink nucleation should predominantly generate xy kinks at low fields and yz kinks at high fields. Harada et al. (1981) have referred to this effect as a switching of the hard anisotropy axis, from the z-axis to the x-axis, as B increases. Also, at the critical field, the in-plane and out-of-plane spin waves at the zone boundaries have equal energies. Thus this switching occurs in both the linear and

nonlinear modes. Evidence from neutron scattering experiments exists for this crossover effect in the linear spin waves in TMMC (Heilmann et al. 1979). Also, there is further high field evidence for this switching effect in the nonlinear modes (Boucher et al. 1984).

The theory of both linear and nonlinear modes will be reviewed here. First the classical antiferromagnetic ground state will be determined. The linear spin wave dispersion relation will be derived by assuming a small amplitude perturbation from the ground state. Then the theory of both xy and yz kinks will be described, with some improvements made over previous work for the yz kink. By using a coordinate system where the polar axis is in the applied field direction, a smoother yz kink profile is obtained. Linear stability analysis for the static yz kink demonstrates an instability at fields less than the critical field. For moving yz kinks, it is shown that the stability is determined by the field and the velocity, and that kink stability is in a sense direction dependent. Actually, the yz kink maintains its stability by tipping the spins toward the applied field, thereby reducing the magnetic field energy. The spin tipping direction (towards or away from the field) and sign of the kink velocity are related.

For the yz kink limit of the equations of motion, a dynamic sine-Gordon equation is obtained, allowing the linear stability analysis to be performed for arbitrary velocity kinks. For the xy kink limit a sine-Gordon equation is obtained only for the static kink, so the arbitrary velocity kink cannot be found. Stability equations can be set up only for the static xy kink. However, a solution to those equations has not yet been found. To text xy kink stability, one must again resort to numerical

simulation, to be described in the next chapter. Also Chapter 6 will introduce a geometrically motivated Ansatz for a general kink excitation, which has xy and yz kinks as limiting cases.

5.3 Classical Antiferromagnetic Ground State

First the classical antiferromagnetic ground state will be determined, since it has a bearing on the zero of energy for kink traveling waves, as well as being necessary for formulation of the Ansatz to be described later.

Nearest neighbor spins tend to be antiparallel in order to minimize the exchange energy. In the absence of an applied field, the ground state is infinitely degenerate, having all spins on the odd lattice sites exactly antiparallel to all the spins on the even lattice sites, with the spin at the origin pointing in an arbitrary direction within the easy plane. The presence of an applied field $B_x \neq 0$ breaks this symmetry; however, we can still use the idea of two sublattices. Let all odd lattice sites comprise the "A" sublattice, and all even lattice sites comprise the "B" sublattice. The ground state should be uniform with the entire A sublattice at some angle to the entire B sublattice. If $\vec{S}_A$ and $\vec{S}_B$ represent the two sublattice vectors, write

$$\vec{S}_A = (x_A, y_A, z_A) \quad , \quad \text{with} \quad x_A^2 + y_A^2 + z_A^2 = S^2 \quad , \tag{5-2a}$$

$$\vec{S}_B = (x_B, y_B, z_B) \quad , \quad \text{with} \quad x_B^2 + y_B^2 + z_B^2 = S^2 \quad , \tag{5-2b}$$

Then the energy per spin is

$$\varepsilon = \frac{1}{2}\{2J(x_A x_B + y_A y_B + z_A z_B) + a(z_A^2 + z_B^2) - g\mu_B B_x(x_A + x_B)\} \quad . \tag{5-3}$$

To minimize ε subject to the constraints in equation (5-2), use Lagrange multipliers ℓ_A and ℓ_B, and extremize

$$q = \varepsilon - \ell_A(x_A^2 + y_A^2 + z_A^2) - \ell_B(x_B^2 + y_B^2 + z_B^2) \quad . \tag{5-4}$$

Taking the partial derivatives $\partial q/\partial x_A = 0$, etc., leads to

$$\begin{aligned}
&Jx_B - \tfrac{1}{2}g\mu_B B_x - 2\ell_A x_A = 0 \\
&Jx_A - \tfrac{1}{2}g\mu_B B_x - 2\ell_B x_B = 0 \\
&Jy_B - 2\ell_A y_A = 0 \\
&Jy_A - 2\ell_B y_B = 0 \\
&Jz_B + Az_A - 2\ell_A z_A = 0 \\
&Jz_A + Az_B - 2\ell_B z_B = 0 \quad .
\end{aligned} \tag{5-5}$$

This is three decoupled two-variable systems. The miminum energy solution is found by taking $z_A = z_B = 0$, which mimimizes the anisotropy energy. Then for $y_A \neq 0$, we require $J^2 = 4\ell_A\ell_B$, and we find the solution

$$x_A = x_B = g\mu_B B_x/4J \tag{5-6a}$$

$$y_A = -y_B = [S^2 - (g\mu_B B_x/4J)^2]^{1/2} \quad . \tag{5-6b}$$

Therefore, the "spin-flopped" ground state is given by

$$\vec{S}_A = S(\tfrac{1}{4}\beta,\ (1 - \beta^2/16)^{1/2} \quad ,\ 0) \tag{5-7a}$$

$$\vec{S}_B = S(\tfrac{1}{4}\beta,\ -(1 - \beta^2/16)^{1/2} \quad ,\ 0) \quad , \tag{5-7b}$$

with energy per spin,

$$\varepsilon_0 = -JS^2(1 + \tfrac{1}{8}\beta^2) \quad , \tag{5-8}$$

where

$$\beta \equiv g\mu_B B_x/JS \quad . \tag{5-9}$$

Note that another solution is obtained by interchanging the A and B sublattices; the ground state is two-fold degenerate.

This is not the only solution of equations (5-5). Two more solutions are obtained by taking $y_A = y_B = 0$. These solutions are

$$\vec{S}_A = S(\beta/(4-\alpha) \quad , \quad 0 \quad , \quad [1 - \beta^2/(4-\alpha)^2]^{1/2}) \tag{5-10a}$$

$$\vec{S}_B = S(\beta/(4-\alpha) \quad , \quad 0 \quad , \quad -[1 - \beta^2/(4-\alpha)^2]^{1/2}) \tag{5-10b}$$

$$\varepsilon = -JS^2[1 - \tfrac{1}{2}\alpha + \tfrac{1}{2}\beta^2/(4-\alpha)] \tag{5-10c}$$

and

$$\vec{S}_A = S(-\beta/\alpha, \quad 0, \quad (1 - \beta^2/\alpha^2)^{1/2}) \tag{5-11a}$$

$$\vec{S}_B = S(-\beta/\alpha, \quad 0, \quad (1 - \beta^2/\alpha^2)^{1/2}) \tag{5-11b}$$

$$\varepsilon = +JS^2(1 + \tfrac{1}{2}\alpha + \tfrac{1}{2}\beta^2/\alpha) \quad , \tag{5-11c}$$

where

$$\alpha \equiv 2A/J \tag{5-12}$$

Solution (5-10) is a local minimum of the energy, but for small α it is not the absolute minimum. Solution (5-11) is an obvious maximum, since the sublattices are parallel. So we conclude that the ground state is described by the spin-flopped configuration (5-7), or its equivalent with A and B interchanged.

5.4 Dynamics: Spin Waves

The spin wave dispersion will be derived, by linearizing the discrete equations of motion resulting from (5-1) about the classical antiferromagnet ground state. In terms of in-plane and out-of-plane angles ϕ_n and θ_n, the ground state sublattices are given by

$$\vec{S}_{\substack{A \\ B}} = S(\cos\phi_0, \pm\sin\phi_0, 0) \tag{5-13a}$$

where

$$\cos\phi_0 = \frac{1}{4}\beta \quad . \tag{5.13b}$$

A small amplitude displacement $(\tilde{\theta}_n, \tilde{\phi}_n)$ from the ground state is assumed, such that

$$\phi_n = \phi_0 + \tilde{\phi}_n \quad n \text{ odd}$$

$$= -\phi_0 + \tilde{\phi}_n \quad n \text{ even} \tag{5-14a}$$

$$\theta_n = \tilde{\theta}_n \qquad \text{all } n \quad . \tag{5-14b}$$

Then under the assumption $\tilde{\theta}_n$, $\tilde{\phi}_n \ll 1$, the discrete equations of motion (see equations (2-5), with $J \to -J$) become

$$(\hbar/JS)\dot{\tilde{\phi}}_n = \tilde{\theta}_{n+1} + \tilde{\theta}_{n-1} + (2+\alpha)\tilde{\theta}_n \tag{5-15a}$$

$$(\hbar/JS)\dot{\tilde{\theta}}_n = (1 - \tfrac{1}{8}\beta^2)(\tilde{\phi}_{n+1} + \tilde{\phi}_{n-1}) - 2\tilde{\phi}_n \quad . \tag{5-15b}$$

A solution is a traveling wave with wavevector k and frequency ω,

$$\tilde{\phi}_n = \Phi e^{i(kna-\omega t)} \tag{5-16a}$$

$$\tilde{\theta}_n = \theta e^{i(kna-\omega t)} \quad , \tag{5-16b}$$

for which one easily finds the dispersion relation

$$(\hbar\omega)^2 = (2JS)^2[1 - (1 - \tfrac{1}{8}\beta^2)\cos ka]\,(1 + \tfrac{1}{2}\alpha + \cos ka) \quad , \tag{5-17}$$

where a is the lattice spacing. Equation (5-17) is plotted in Figure 5.1 for various α and β. The limits at the zone boundaries are

$$(\hbar\omega)^2 = (JS)^2[\beta^2 + 4(ka)^2] \quad , \quad \text{near } ka = 0 \tag{5-18a}$$

$$(\hbar\omega)^2 = (2JS)^2[\alpha + (ka-\pi)^2] \quad , \quad \text{near } ka = \pi \quad . \tag{5-18b}$$

These spin wave energies at the zone boundaries are exactly equal when $4\alpha = \beta^2$, which gives the critical field $B_c = (8AJS^2)^{1/2}$. Near ka = 0, the relative amplitudes of $\tilde{\theta}_n$ and $\tilde{\phi}_n$ are given by

$$-i\beta\Phi \lesssim (4+\alpha)\theta \quad . \tag{5-19}$$

Since α, $\beta \ll 4$ for moderate fields and most real materials, we have $\Phi \gg \theta$, so that this is an in-plane mode, whose energy depende only on β, since the motion is against the applied field. Near $ka = \pi$, the relative amplitudes are given by

$$-2i\Phi \lesssim \alpha^{1/2}\theta \quad . \tag{5-20}$$

Since $\alpha \ll 4$ ($\alpha \lesssim 0.04$ for TMMC), we now have $\theta \gg \Phi$, and this is an out-of plane mode whose energy depends only on α, as expected. For both modes the $\tilde{\theta}_n$ and $\tilde{\phi}_n$ motions are 90° out of phase. These modes are closely related to the kink modes of the system. It will be shown below that the in-plane spin wave energy (at ka = 0, quantized) is equal to the in-plane <u>static</u> kink energy, and similarly the out-of-plane spin wave energy (at $ka = \pi$, quantized) is equal to the out-of-plane static kink energy.

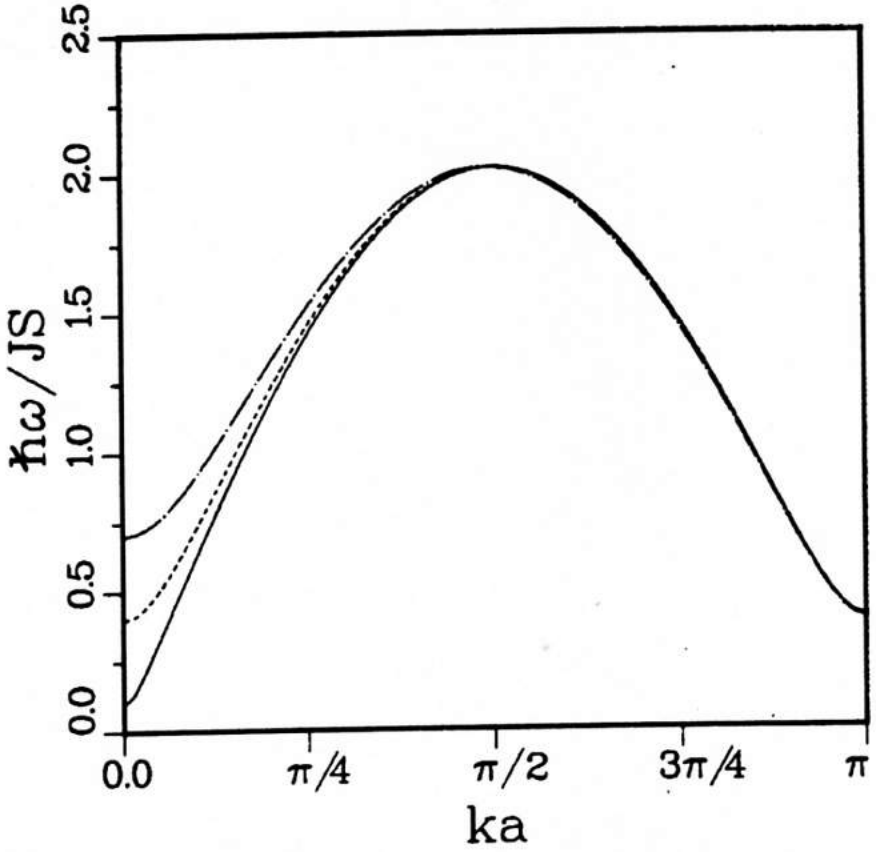

Fig. 5.1 Antiferromagnet spin wave dispersion relationship (equation 5-17) for $\alpha = 0.04$, and applied fields $\beta = g\mu_B B/JS = 0.1$ (solid), $\beta = 0.4$ (dashed, the critical field) and $\beta = 0.7$ (chained). Note that the frequencies at the zone boundaries are equal when $\beta = \beta_c \equiv 2\alpha^{\frac{1}{2}}$.

5.5 Dynamics: The Continuum Limit

First, the continuum limit equations of motion resulting from (5-1) will be derived, as given by Mikeska (1980) and Flüggen and Mikeska (1983). The spin variables on the A and B sublattices are parametrized in terms of four angles in spherical polar coordinates:

$$\vec{S}_{\substack{A\\B}} = \pm S(\sin(\Theta\pm\theta)\cos(\Phi\pm\phi),\ \sin(\Theta\pm\theta)\sin(\Phi\pm\phi),\ \cos(\Theta\pm\theta)). \tag{5-21}$$

The angles Θ, Φ, θ and ϕ are all functions of position z and time t. Angles Θ and Φ are considered large compared to the small angles θ and ϕ. To go to the continuum limit (of equations (2-5)), slow spatial variations in Θ and Φ are assumed, in addition to θ, $\phi \ll 1$. Measuring time in units of $\hbar/JS$, and using the lattice constant a as the length unit, the evolution equations are

$$\dot{\Theta} = 4\phi \sin\Theta + \beta \sin\Phi \tag{5-22a}$$

$$\dot{\Phi} = -4\theta \csc\Theta + \beta \cot\Theta \cos\Phi - \alpha\theta \sin\Theta \tag{5-22b}$$

$$\dot{\theta} = -4\phi\theta\cos\Theta - 2\Theta_z\Phi_z - \Phi_{zz}\sin\Theta + \beta\phi \cos\Phi \tag{5-22c}$$

$$\dot{\phi} = 4\theta^2\cos\Theta \csc^2\Theta - (4\phi^2 + \Phi_x^2)\cos\Theta + \Theta_{zz}\csc\Theta + \alpha(1 - \tfrac{1}{2}\theta^2)\cos\Theta$$
$$- \beta(\phi\cot\Theta \sin\Phi + \theta\csc^2\Theta \cos\Phi) \quad . \tag{5-22d}$$

Subscripts denote partial derivatives. The small angles can be eliminated by solving (5-22a) and (5-22b), assuming $\alpha \ll 4$:

$$\theta = \tfrac{1}{4}(\beta \cos\Theta \cos\Phi - \dot{\Phi} \sin\Theta) \tag{5-23a}$$

$$\phi = \tfrac{1}{4} \csc\Theta(\dot{\Theta} - \beta \sin\Phi) \quad . \tag{5-23b}$$

Inserting these back into (5-22c) and (5-22d) leads to equations involving only the large angles Θ and Φ,

$$(\Phi_{zz} - \tfrac{1}{4}\ddot{\Phi})\sin\Theta + 2(\Theta_z\Phi_z - \tfrac{1}{4}\dot{\Theta}\dot{\Phi})\cos\Theta = -\tfrac{1}{4}\beta^2\sin\Theta\sin\Phi\cos\Phi + \tfrac{1}{2}\beta\dot{\Theta}\sin\Theta\cos\Phi \qquad (5\text{-}24a)$$

$$(\Theta_{zz} - \tfrac{1}{4}\ddot{\Theta})\csc\Theta - (\Phi_z^2 - \tfrac{1}{4}\dot{\Phi}^2)\cos\Theta = (\tfrac{1}{4}\beta^2\cos^2\Phi - \alpha)\cos\Theta - \tfrac{1}{2}\beta\dot{\Phi}\sin\Theta\cos\Phi \quad . \qquad (5\text{-}24b)$$

In principle these equations govern the dynamics completely. In practice, it will be seen that although they give a sG equation for the out-of-plane kinks, the kink profile obtained has a cusp which makes it a poor solution for the original Hamiltonian. This problem will be avoided by choosing the x-axis to be the polar axis. For the in-plane kinks, however, equation (5-24) is adequate, especially since the in-plane kink involves rotation of the spins in the xy plane, about the polar z-axis.

5.6 xy (in-plane) sine-Gordon Kinks

Statically, equation (5-24b) is satisfied exactly when $\Theta = \frac{1}{2}\pi$. Equation (5-23a) then becomes a static sG equation for the variable $\psi = 2\Phi - \pi$. More generally, Mikeska (1980) has assumed $\Theta = \frac{1}{2}\pi - \Theta_s$, where $\Theta_s \ll 1$; then linearizing in Θ_s leads to a dynamic sG equation for ψ, depending on the parameter β,

$$\psi_{zz} - \tfrac{1}{4}\ddot{\psi} = \tfrac{1}{4}\beta^2\psi \quad , \qquad (5.25a)$$

with Θ_s satisfying

$$(\Theta_{szz} - \tfrac{1}{4}\ddot{\Theta}_s) + (\Phi_z^2 - \tfrac{1}{4}\dot{\Phi}^2 + \tfrac{1}{4}\beta^2\cos^2\Phi - \alpha)\Theta_s = \tfrac{1}{2}\beta\dot{\Phi}\cos\Phi \quad . \qquad (5\text{-}25b)$$

Note that the speed of "sound" is c = 2 in these units. At low fields $\beta^2 \ll 4\alpha$, and ignoring the second derivatives of Θ_s in (5-25b), the xy kink solution is a π rotation in the xy plane, moving as a traveling wave at velocity v,

$$\Phi = \frac{1}{2}\pi + 2\tan^{-1}\exp\tilde{x} \quad ; \quad \tilde{x} \equiv \frac{1}{2}\gamma\beta(z - vt) \quad , \tag{5-26a}$$

$$\Theta_s \simeq -\frac{1}{4}(\beta^2\gamma v/\alpha)\mathrm{sech}^2\tilde{x} \quad ; \quad \gamma \equiv (1 - \frac{1}{4}v^2)^{-1/2} \quad . \tag{5-26b}$$

A typical xy kink profile from equation (5-26) is shown in Figure 5.2. In the general case for arbitrary field compared to anisotropy, one must solve

$$(\Theta_{szz} - \frac{1}{4}\ddot{\Theta}_s) + (\frac{1}{2}\beta^2\mathrm{sech}^2\tilde{x} - \alpha)\Theta_s = \frac{1}{4}\beta^2\gamma v\ \mathrm{sech}^2\tilde{x} \tag{5-27}$$

in order to get Θ_s. A solution for this equation has not yet been found, but it would give the kink profile for arbitrary α and β in the small Θ_s approximation.

For solution (5-26), the kink energy can be evaluated using the continuum limit Hamiltonian

$$H = \frac{1}{2}JS^2 \int dz\{\theta_z^2 + 4\theta^2 + (\phi_z^2 + 4\phi^2)\sin^2\theta\}$$

$$+ AS^2 \int dz\{\cos^2\theta - \theta^2\cos 2\theta\}$$

$$-g\mu_B B_x S \int dz\ \{\theta\cos\theta\cos\Phi - \phi\sin\theta\sin\Phi\} \quad . \tag{5-28}$$

The xy kink energy is found to be

$$E_{xy} = (JS^2)(\gamma\beta) \quad . \tag{5-29}$$

Small corrections to the pure sG energy have been dropped, although this result is valid for arbitrary α and β, assuming the profile used is a good

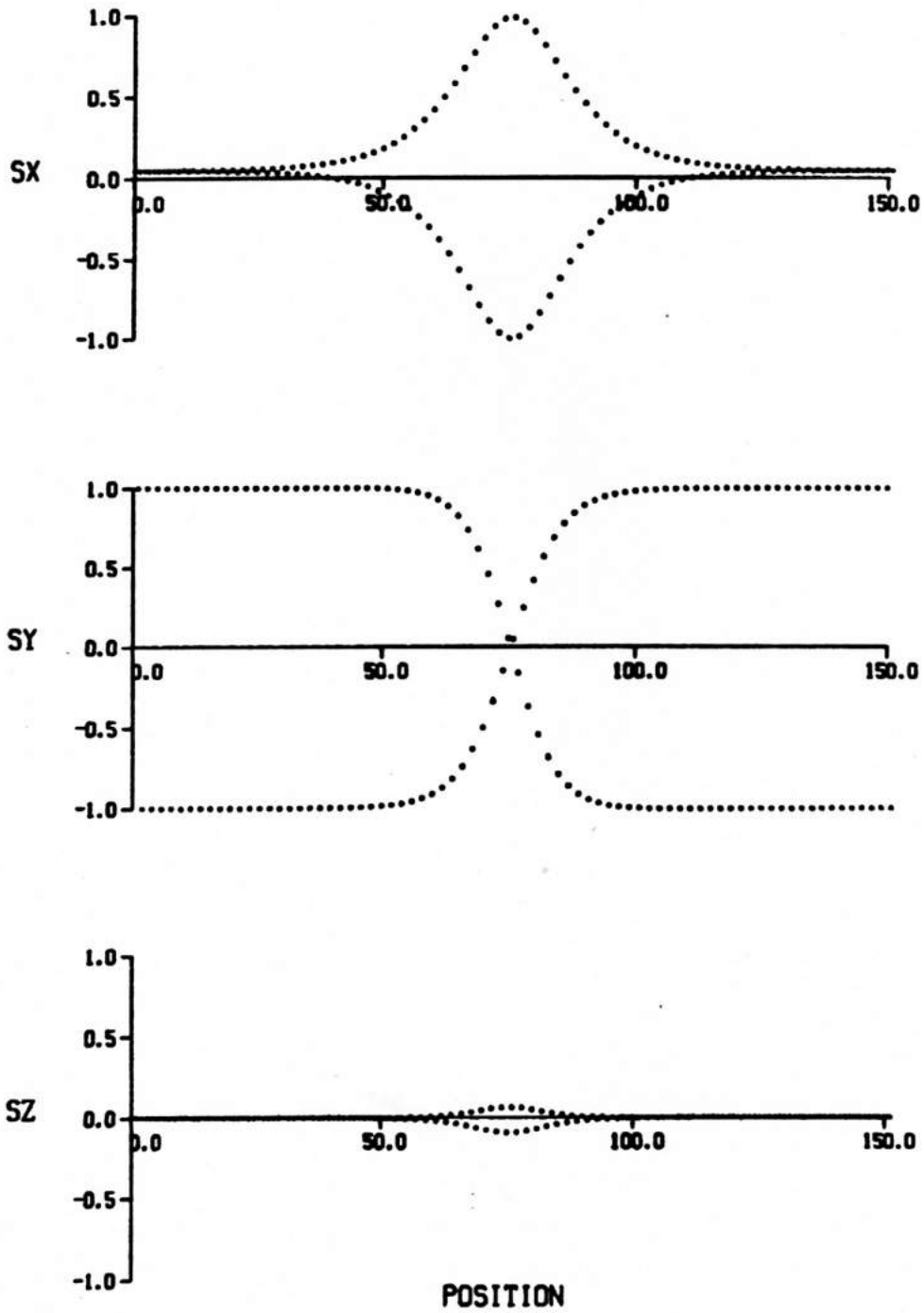

Figure 5.2 A typical xy sG kink profile, equation 5-26, in xyz spin components, for $\alpha = 0.04$, $\beta = 0.20$, $v/c = 0.3$

solution. We will see later from the numerical simulation and the Ansatz calculation that the sign of the curvature of E_{xy} reverses at the critical field defined by $\beta_c^2 = 4\alpha$. It is suggested that there is a kind of xy kink instability at $\beta = \beta_c$, reminiscent of that in the ferromagnet. A kink with energy decreasing as a function of velocity as here and for the branch III ferromagnetic kinks, implies a negative effective mass. For $\beta^2 > 4\alpha$, E_{xy} has this behavior, and we suggest that in this regime the xy kinks are analogous to the branch III ferromagnetic backwards moving kinks. This will be made clearer later. Also, if an exact solution for Θ_s for arbitrary α and β were available then the instability in E_{xy} would be obvious. The situation for yz (out-of-plane) kinks is much clearer, and is discussed next.

5.7 yz (out-of-plane) sine-Gordon Kinks

Equation (5-24a) is satisfied exactly by $\Phi = \frac{1}{2}\pi$, in which case (5-23b) becomes the sG equation for the variable $2\Theta-\pi$, depending on the parameter α:

$$\Theta_{zz} - \frac{1}{4}\ddot{\Theta} = -\alpha \sin\Theta\cos\Theta \quad . \tag{5-30}$$

The dynamic kink solution is a π notation in the yz plane,

$$\Theta = \frac{1}{2}\pi + 2\tan^{-1}\exp x \qquad x \equiv \gamma\sqrt{\alpha}(z-vt) \quad . \tag{5-31}$$

This is an exact result in the small angle approximation (θ, $\phi \ll 1$), but upon solving for θ and ϕ, one obtains

$$\theta = 0 \tag{5-32a}$$

$$\phi = \frac{1}{4}(\gamma\sqrt{\alpha}\ v\ \mathrm{sech}\ x + \beta)\coth x \quad . \tag{5-32b}$$

At the center of the kink (x = 0), ϕ is no longer small as assumed, and this solution is not valid. The profile has an unphysical cusp in S^x which prohibits its use as initial conditions in numerical simulations. A typical profile is given in Figure 5.3. Thus we need a different approach.

The problem can be corrected by using a more appropriate coordinate system. Spherical polar coordinates where the x-axis is the polar axis exploit the symmetry of yz kinks; therefore the spins are re-parameterized (Wysin et al. 1985) in terms of <u>new</u> angles Θ, Φ, θ, and ϕ in <u>x-polar</u> spherical coordinates

$$\vec{S}_{\substack{A\\B}} = \pm S(\cos(\Theta\pm\theta),\ \sin(\Theta\pm\theta)\cos(\Phi\pm\phi),\ \sin(\Theta\pm\theta)\sin(\Phi\pm\phi)) \quad . \tag{5-33}$$

The dynamical equations are now

$$\dot{\Theta} = 4\phi\ \sin\Theta + \alpha(\phi\ \sin\Theta\ \cos 2\Phi + \tfrac{1}{2}\theta\ \cos\Theta\ \sin 2\Phi) \tag{5-34a}$$

$$\dot{\Phi} = -4\theta\ \csc\Theta + \alpha(\theta\ \sin\Theta\ \sin^2\Phi - \phi\ \cos\Theta\ \sin 2\Phi) - \beta \tag{5-34b}$$

$$\dot{\theta} = -(2\Phi_z\Theta_z + 4\theta\phi)\cos\Theta - \Phi_{zz}\sin\Theta + \tfrac{1}{2}\alpha\ \sin\Theta\ \sin 2\Phi \tag{5-34c}$$

$$\dot{\phi} = -(4\phi^2 + \Phi_z^2 - 4\theta^2\csc^2\Theta)\cos\Theta + \Theta_{zz}\csc\Theta - \alpha\cos\Theta\ \sin^2\Phi \quad . \tag{5-34d}$$

Once again, with the assumption $\alpha \ll 4$, the small angles can be eliminated, leading to dynamical equations involving only the large angles Θ and Φ, similar to equation (5-24),

$$(\Phi_{zz} - \tfrac{1}{4}\ddot{\Phi})\sin\Theta + 2(\Theta_z\Phi_z - \tfrac{1}{4}\dot{\Theta}\dot{\Phi})\cos\Theta = \tfrac{1}{2}\alpha\sin\Theta\sin 2\Phi + \tfrac{1}{2}\beta\dot{\Theta}\cos\Theta \tag{5-35a}$$

$$(\Theta_{zz} - \tfrac{1}{4}\ddot{\Theta})\csc\Theta - (\Phi_z^2 - \tfrac{1}{4}\dot{\Phi}^2)\cos\Theta = (\alpha\sin^2\Phi - \tfrac{1}{4}\beta^2)\cos\Theta - \tfrac{1}{2}\beta\dot{\Phi}\cos\Theta \quad , \tag{5-35b}$$

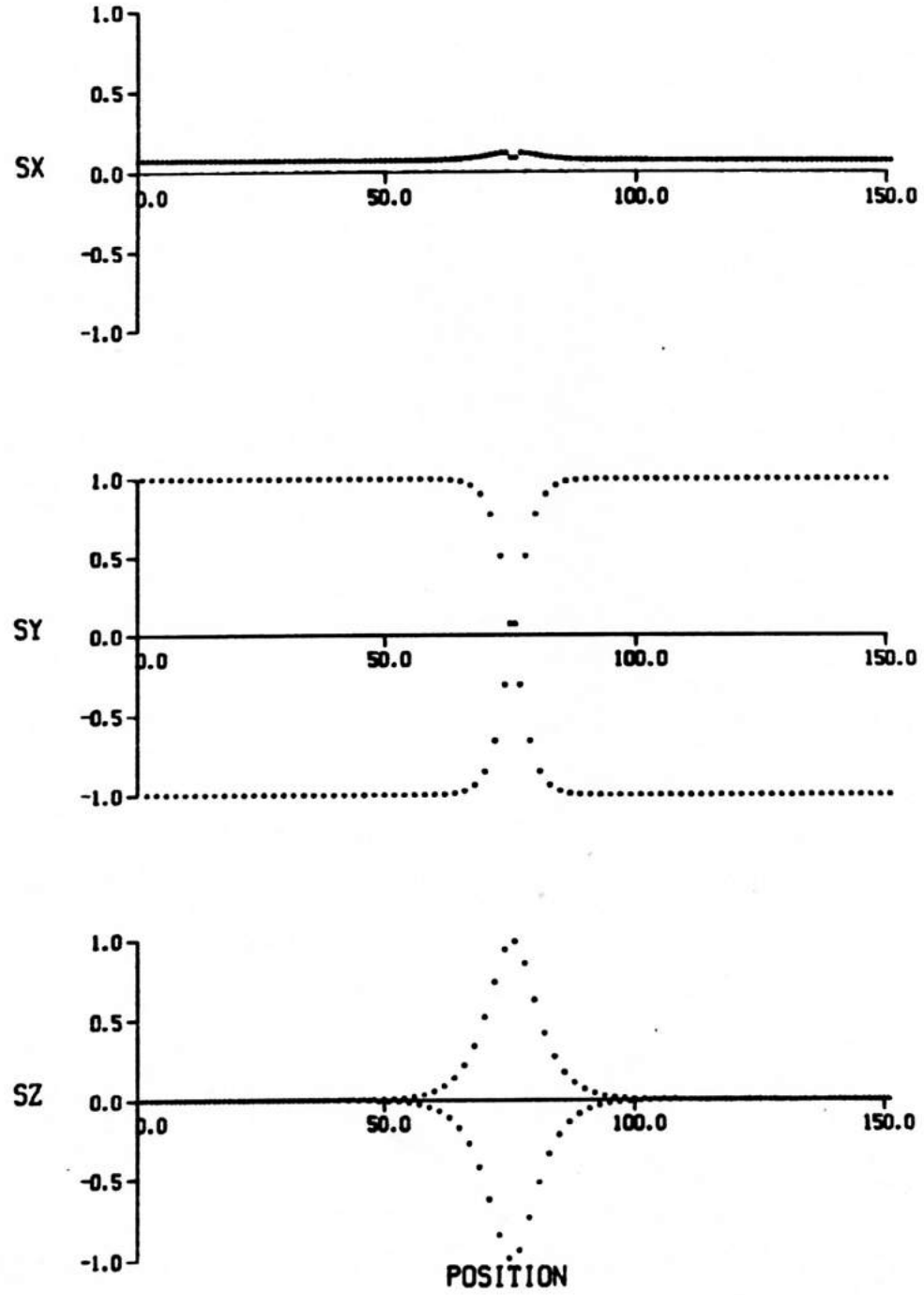

Figure 5.3 A typical yz sG kink profile in xyz spin components, as obtained using z-polar spherical coordinates, equations 5-31 and 5-32, for $\alpha = 0.04$ $\beta = 0.3$ and $v/c = 0.5$. The kink has been centered between grid points. This is not a good traveling wave solution, due to the cusp in S^x.

with the small angles given as

$$\theta = -\frac{1}{4}(\beta + \dot{\Phi})\sin\theta \tag{5-36a}$$

$$\phi = \frac{1}{4}\dot{\theta}\csc\theta \quad . \tag{5-36b}$$

Now to look for a yz kink solution, note that $\Theta = \frac{1}{2}\pi$ exactly satisfies (5-35b), and then (5-35a) becomes a dynamic sG equation for 2Φ,

$$(2\Phi)_{zz} - \frac{1}{4}(2\ddot{\Phi}) = \alpha\sin 2\Phi \quad . \tag{5-37}$$

The yz kink solution is given by

$$\Theta_0 = \frac{1}{2}\pi \tag{5-38a}$$

$$\Phi_0 = 2\tan^{-1}\exp x \tag{5-38b}$$

$$\theta_0 = -\frac{1}{4}(\beta - \gamma\sqrt{\alpha}\ v\ \mathrm{sech}\ x) \tag{5-38c}$$

$$\phi_0 = 0 \quad , \tag{5-38d}$$

with x as previously defined in equation (5-31). A typical yz kink profile from (5-38) is given in Figure 5.4. This is a smooth profile, and has been used in numerical simulations as initial conditions. This is an improvement over the kink profile in z-polar coordinates as derived by Fluggen and Mikeska (1983), equations (5-31) and (5-32).

The continuum Hamiltonian in x-polar coordinates is

$$\begin{aligned} H = {} & \frac{1}{2} JS^2 \int dz\ \{\theta_z^2 + 4\theta^2 + (\Phi_z^2 + 4\phi^2)\sin^2\theta\} \\ & + AS^2 \int dz\{(\sin^2\theta + \theta^2\cos 2\theta)(\sin^2\Phi + \phi^2\cos\Phi) + 2\theta\phi\sin 2\theta\sin 2\Phi\} \\ & - g\mu_B B_x S \int dz\ \sin\theta\sin\theta \quad . \end{aligned} \tag{5-39}$$

Then the yz kink energy is found to be

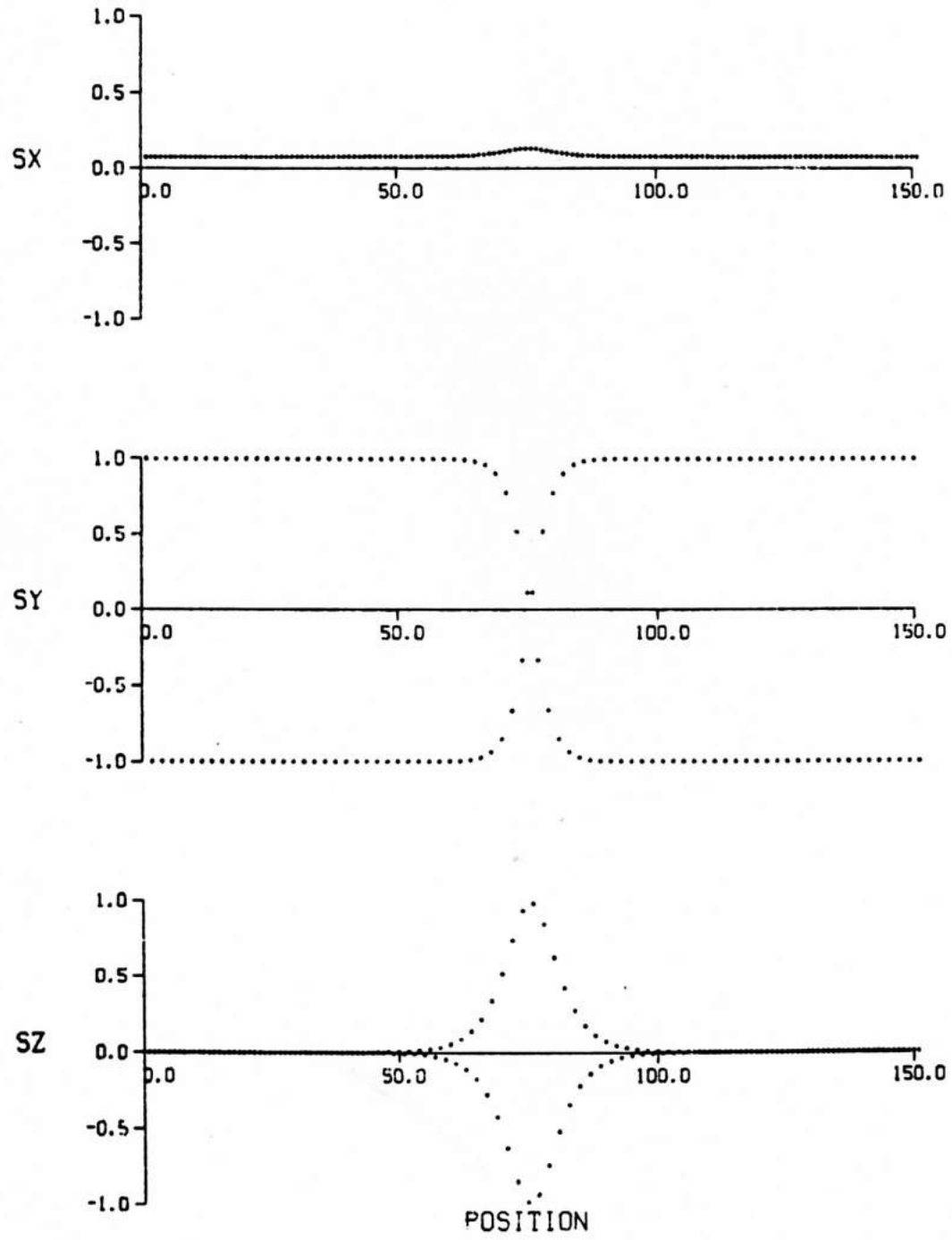

Figure 5.4 A typical yz sG kink profile in xyz spin components, as obtained using x-polar spherical coordinates, equation 5-38, for $\alpha = 0.04$, $\beta = 0.03$ and $v/c = 0.5$. This is a smooth function compared to that of Figure 5.3.

$$E_{yz} = 2\gamma\sqrt{\alpha}[1 - \frac{\beta^2}{32}(1 - \frac{1}{4}v^2)] \quad . \tag{5-40}$$

The instability which was apparent from E_{xy} is not apparent here. In the next section we see that there is a true structure instability in static yz kinks at the critical field, defined by $\beta_c^2 = 4\alpha$.

A comment is in order concerning how a positive velocity yz kink differs physically from a negative velocity yz kink. The physical polar angles θ_n measured from the x-axis on the A and B sublattices (not the field θ) are, from (5-33) and (5-38),

$$\theta_A = \Theta_0 + \theta_0 = \frac{1}{2}\pi - \frac{1}{4}\beta + \frac{1}{4}\beta\gamma\sqrt{\alpha}\ v\ \text{sech}\ x \tag{5-41a}$$

$$\theta_B = \pi - (\Theta_0 - \theta_0) = \frac{1}{2}\pi + \theta_0 = \theta_A \quad . \tag{5-41b}$$

The polar angles for both sublattices are equal, by symmetry. So we see that for positive v, the spins are canted away from the field, while for negative v the spins are canted toward the field (when compared to the static kink). We will see later how this fact relates to the linear stability analysis for moving yz kinks.

5.8 yz Kinks: Linear Stability Analysis in x-polar Coordinates

The linear stability analysis for the yz kinks is straightforward. We assume small perturbations $\tilde{\Theta}$, $\tilde{\Phi}$, $\tilde{\theta}$ and $\tilde{\phi}$ about the exact sG kink solution Θ_0, Φ_0, θ_0, ϕ_0, substitute into equations of motion (5-34), and linearize in these perturbations. Again, with $\alpha \ll 4$, the small angles $\tilde{\theta}$ and $\tilde{\phi}$ can be eliminated, and the resulting decoupled stability equations

for $\tilde{\Theta}$ and $\tilde{\Phi}$ are

$$\tilde{\theta}_{zz} + (\phi_{0z}^2 - 4\theta_0^2 + \alpha\sin^2\phi_0)\tilde{\theta} = \tfrac{1}{4}\ddot{\tilde{\theta}} \tag{5-42a}$$

$$\tilde{\phi}_{zz} - (\alpha\cos 2\phi_0)\tilde{\phi} = \tfrac{1}{4}\ddot{\tilde{\phi}} \quad . \tag{5-24b}$$

Using the known ϕ_0 and θ_0, and assuming $\tilde{\theta} \sim e^{i\omega_1 t}$ and $\tilde{\phi} \sim e^{i\omega_2 t}$ time dependences, yields the following eigenvalue problems:

$$-\gamma^2\tilde{\theta}_{xx} + (1 - 2\operatorname{sech}^2 x - \frac{\beta\gamma v}{2\sqrt{\alpha}}\operatorname{sech} x)\tilde{\theta} = \lambda_1\tilde{\theta} \tag{5-43a}$$

$$-\gamma^2\tilde{\phi}_{xx} + (1 - 2\operatorname{sech}^2 x)\tilde{\phi} = \lambda_2\tilde{\phi} \quad , \tag{5-34b}$$

where the eigenvalues λ_1 and λ_2 are related to the eigenfrequencies ω_1 and ω_2 by

$$\omega_1^2 = 4\alpha(\lambda_1 - 1) + \beta^2 \tag{5-44a}$$

$$\omega_2^2 = 4\alpha\lambda_2 \quad . \tag{5-44b}$$

For a static kink ($v = 0$) these equations are identical; bound state solutions are given by sech x, with eigenvalues $\lambda_1 = \lambda_2 = 0$. Then the corresponding eigenfrequencies are

$$\omega_1^2 = \beta^2 - 4\alpha \tag{5-45a}$$

$$\omega_2^2 = 0 \quad . \tag{5-45b}$$

The zero frequency bound state associated with $\tilde{\Phi}$ is the Goldstone translation mode, reflecting the fact that the kink can shift its position with no change in energy. There is no instability implied by this mode. The bound state associated with $\tilde{\Theta}$, however, in general has a nonzero

frequency, which becomes imaginary for $\beta^2 < 4\alpha$, indicating unstable $\exp(|\omega_2|t)$ time dependence. Therefore we have shown that at low fields below β_c, static yz kinks are unstable, and the mode responsible for this instability causes the spins to tilt away from the z-axis. This result has been confirmed by numerical simulation, to be discussed in the next chapter.

For nonzero velocity v, the "potential" in (5-43a) for $\tilde{\theta}$ is modified, and therefore so is the eigenvalue λ_1. The interesting point here is that the potential becomes <u>deeper</u> if v is positive, and therefore one expects λ_1 to be decreased below zero. Since the stability criterion is $\beta^2 > 4\alpha(1-\lambda_1)$ (from $\omega_1^2 > 0$), we conclude that a positive velocity kink requires a <u>larger</u> field to be stable than does the static kink. If the velocity is negative, however, then λ_1 is greater than zero, and a <u>smaller</u> field is necessary for stability. So even for $\beta < \beta_c$, there can be <u>stable moving</u> yz kinks. Motion can enhance or diminish yz kink stability.

These comments can be made quantitative by solving for $\lambda_1(v)$ using first order perturbation theory. A simple calculation shows that λ_1 becomes

$$\lambda_1(v) \simeq \frac{1}{3}(\gamma^2-1) - \frac{\pi\gamma\beta}{8\sqrt{\alpha}}\, v \quad . \tag{5-46}$$

To get an expression <u>correct</u> to order v^2, one needs to go to second order perturbation theory. This calculation has been done, but the results differ from the first order results by only a few per cent for fields near the critical field. Keeping terms only to first order in v, then, the stability criterion $\omega_1^2 > 0$ for moving yz kinks is approximately given by

$$\frac{v}{c} < \frac{\beta^2-4\alpha}{\pi\beta\sqrt{\alpha}} \quad , \tag{5-47}$$

where $c = 2$ is the long wavelength spin wave velocity (in these units). The numerical simulations to be described in Chapter 6 give stability results consistent with this relationship.

There seems to be an asymmetry here, implied by this direction-dependent stability. But there is none. Note that there is another yz kink solution, as well as two antikink solutions to equation (5-37), if we consider a "kink" to be a counterclockwise rotation in the yz plane and an "antikink" to be a clockwise rotation. The <u>other</u> kink

$$\Phi_0' = \pi + 2 \tan^{-1}\exp x \quad . \tag{5-48}$$

Shifting Φ by π changes θ to

$$\theta_0' = -\frac{1}{4}(\beta - \gamma\sqrt{\alpha}\, v \operatorname{sech} x) \quad . \tag{5-49}$$

It is obvious that following through the stability analysis for <u>this</u> solution, the <u>negative</u> velocity kink will be found to be more stable than the <u>positive</u> velocity kink, opposite to what was found for kink solution (5-38). However, in <u>both</u> cases, it is seen that the more stable direction is the one where the spins are canted further toward the field. The same is true for the antikinks, which are obtained from the expressions for the kinks by changing $x \rightarrow -x$. Therefore, it is concluded that the canting of the spins toward the field enhances the stability of yz kinks (or antikinks). Furthermore, yz kink stability is determined by both the applied field <u>and</u> the kink velocity, for fixed α.

For static xy kinks, it is not yet possible to generally solve the relevant stability equations, since the small angles do not decouple from the large angles as for yz kinks. Therefore we have not been able to make any definite statements about the existence of bound states, nor about the

stability from this analytic viewpoint. The xy kink stability will be tested numerically in Chapter 6.

5.9 Summary

The dispersion relations for linear spin waves, and for nonlinear kink modes have been reviewed. We have seen that for both linear and nonlinear excitations, there is a classification into either in-plane or out-of-plane modes, and that the relative energies of these modes depends on the ratio $\beta^2/4\alpha$. The static nonlinear modes have the same energies as the linear modes at the zone boundaries. At small fields $\beta^2 < 4\alpha$, the in-plane modes have lower energy, while at large fields $\beta^2 > 4\alpha$, the out-of-plane modes have lower energy.

The stability regime for static yz kinks has been found to be $\beta^2 > 4\alpha$. For dynamic yz kinks, the stability is determined by both the applied field and the velocity; stable moving yz kinks have the two sublattices canted toward the field. For xy kinks, we cannot generally perform the same stability analysis even for the static kinks, since the equations for the four variables $\tilde{\Theta}$, $\tilde{\Phi}$, $\tilde{\theta}$ and $\tilde{\phi}$ do not decouple. However, the xy dispersion relation may indicate an instability similar to that seen in easy-plane ferromagnets above the critical field, where the kinks have negative effective mass, and move in the opposite direction from that predicted by sG theory.

The nonlinear xy and yz kink modes have been found as separate sG limits of the equations of motion, written in two different coordinate systems, as dictated by the symmetry of the mode. We will show in Chapter 6 that xy and yz kinks are actually closely related from a geometrical viewpoint, in that they can both be derived from a single variational Ansatz. Also we will perform single kink numerical simula-

tions to test the Ansatz, as well as verify the stability results for yz kinks, and test xy kink stability.